Organic & Biomolecular Chemistry

Accepted Manuscript

This article can be cited before page numbers have been issued, to do this please use: K. Roy, S. Ghosh, M. Chetia, P. Satpati and S. Chatterjee, *Org. Biomol. Chem.*, 2019, DOI: 10.1039/C9OB00014C.

ROYAL SOCIETY OF CHEMISTRY

rsc.li/obc

View Article Online
DOI: 10.1039/C9OB00014C

Dicyclohexylurea derivatives of amino acids as dye absorbent organogels and anion sensors

Karabi Roy,[1] Suvankar Ghosh,[2] Monikha Chetia,[1] Priyadarshi Satpati[2*] and Sunanda Chatterjee[1*]

1. Department of Chemistry,
   Indian Institute of Technology, Guwahati
   Guwahati, Assam, India 781039.
   Email: sunanda.c@iitg.ac.in
   Telephone: 0361-2583310
2. Department of Biosciences and Bioengineering
   Indian institute of technology, Guwahati,
   Guwahati, Assam, India 781039.
   Email: psatpati@iitg.ac.in
   Telephone: 0361-2583205

View Article Online
DOI: 10.1039/C9OB00014C

Abstract:

Dicyclohexyl urea (DCU) derivatives of amino acids Fmoc-Phe-DCU (M1), Fmoc-Phg-DCU (M2) and Fmoc-Gaba-DCU (M3) have been shown to form phase selective, thermoreversible and mechanically robust gels in a large range of organic solvents. This is the first report of low molecular weight gelators (LMWG) from DCU derivatives of amino acids. The self-assembly mechanism of the organogels has been probed using concentration dependent ^{1}H NMR, DMSO titration ^{1}H NMR, Fluorescence, FTIR, PXRD and FESEM techniques. Self-assembly leading to gelation process is mainly driven by hydrophobicity and π-π stacking interactions in between Fmoc groups. Interestingly, the gels can absorb several kinds of organic dyes efficiently and can be reused for dye absorption for multiple cycles. Additionally, M1-M3 act as sensors for anions like fluoride, acetate and hydroxide, for which they have specific fluorescence response. Gel formation by M1-M3 is completely arrested in the presence of fluoride. The possible binding mode of fluoride has been delineated using DFT studies. Calculations suggest, involvement of urea NH in a six membered intramolecular hydrogen bond, rendering it unavailable for fluoride binding. Backbone -NH of the amino acids of M1-M3 is responsible for fluoride binding. The reported small, economically viable, synthetically facile molecules not only enrich the repertoire of LMWG molecules, but can have multifaceted applications.

Keywords: Low molecular weight gelators, urea derivatives, organogels, π-π stacking, dye absorption, water pollution, selective anion sensors, DFT calculations.

Abbreviations:

View Article Online
DOI: 10.1039/C9OB00014C

DCU	Dicyclohexyl urea
Fmoc	Fluorenylmethyloxycarbonyl
FESEM	Field emission scanning electron microscopy
NMR	Nuclear magnetic resonance
FTIR	Fourier transform Infrared spectroscopy
PXRD	Powder X-ray diffraction
LMWG	Low molecular weight gelators
1, 2 DCB	1,2 Dichlorobenzene.
CV	Crystal Violet
RB	Rhodamine B
NR	Neutral red
MGC	Minimum gelation concentration
Phe	Phenylalanine
Phg	Phenyl glycine
Gaba	γ amino butyric acid
RT	Room Temperature
THF	Tetrahydrofuran
DFT	Density functional theory
TDDFT	Time-dependent density function theory
ANS	8-Anilinonapthalene-1-sulfonic acid
DCC	Dicyclohexylcarbodiimide
ACN	Acetonitrile

View Article Online
DOI: 10.1039/C9OB00014C

Introduction:

Low-molecular-weight gelators (LMWG) are small molecules that can immobilize solvents through molecular self-assembly, and represent a novel class of supramolecular functional materials[1-3]. There is a plethora of literature on the various applications[2-3] of LMWG: as templated materials,[4] light harvesting materials,[5]stabilizers of organic photo chromic materials,[6]enzyme-immobilization matrices for *in situ* formation and stabilization of nanoparticles and clusters [7]in preparation of dye sensitized solar cells,[8]dental composite carriers,[9]controlled release of bioactive molecules and drugs;[1038-45] in cell culture and tissue engineering,[11-12] phase selective gelation,[13-15]oil spill recovery,[13-14,16]waste treatment, dye adsorption,[17-22] and others[23-24]. Organogelators are molecules that create a three-dimensional (3D) network in organic solvents by self-organization of the monomeric species to higher-order structures. Gelation is driven by specific non-covalent intermolecular interactions, commonly electrostatic, dipole–dipole, van der Waals, π-π stacking, hydrophobic, hydrogen bonding and hydrophilic-lipophilic balance.[25-27] The diverse applicability of the organogelators have stimulated in the growth of rationally designed small molecules over the last few decades.[28-33]Amino acids and peptides have emerged as one of the potential gelator molecules that are easy to avail, cost effective, biocompatible and capable of forming gels in a wide variety of organic solvents. Though there are a few studies which report gelation of small peptides and single amino acid derivatives,[34-36] there are no reports of dicyclohexyl urea (DCU) derivatives of single amino acids forming organogels.

In this report, we have designed three single amino acid derivatives of DCU namely, Fmoc-Phe-DCU (M1), Fmoc-Phg-DCU (M2) and Fmoc-Gaba-DCU (M3) (Figure 1a) and for the first time reported their organogelation. We have also tried to understand their mechanism of self-assembly and looked at their potential applications.

Water pollution is a matter of grave environmental concern in the modern day society and

View Article Online
DOI: 10.1039/C9OB00014C

treatment of waste water is of primary importance. Dyes used in textile, paper, leather, cosmetics, pharmaceutical and food industries are major sources of water pollution[37] and upon reaching water bodies have adverse effect on all forms of life and on ecosystem as a whole.[38] The dye effluents and their degradation products are toxic and carcinogenic exhibiting negative impact on the immune system, reproductive system and possessing potential geno-toxicity and cardio-toxicity.[39-40] Conventional methods of treating dye effluents like incineration, biological treatment, absorption upon solid matrices like activated carbon, chemical precipitation, electrochemical techniques, ion exchange, and others, have their own limitations due to their low sensitivity, incomplete removal, high-energy requirements, and production of toxic sludge.[41] Hydro/Organogel-based soft materials[17] offer an appealing alternative for removal of dyes from contaminated water due to their high water permeability, large surface area for adsorption and simplicity in use along with reusability and proper biodegradability.

Though anions play a vital role in various environmental and health processes, overexposure may lead to pathological problems. For example, fluoride is extremely important for dental care and osteoporosis, while chronic exposure to high levels of fluoride anion can lead to dental or skeletal fluorosis.[42] Fluorine is also present in several chemical weapons like sarin, soman etc.[43] This makes anion detection, and hence design, synthesis and development of new sensors of immense importance.[44-45] Of the various responses generated upon ion sensing, optical sensors (generating fluorescence response) are the most popular being highly sensitive.[46] Urea moiety is a well-known anion binder.[47] There are several experimental [48] and computational [49-50]studies on urea based fluoride sensors. Development of anion, especially fluoride responsive low molecular weight organogels is an area of active research.[51-55]

In a quest to find suitable applications for organogels M1-M3, we found them to be efficient and recyclable organic dye absorbents. Additionally, molecules M1-M3 can act as sensors of selective anions like fluoride, acetate and hydroxide. Anion sensing abilities of the molecules

have been studied using spectroscopic techniques like UV absorption, fluorescence and NMR on one hand and DFT studies on the other. Such simple, economically viable yet multifunctional small molecules are of immense relevance in the recent times.

Results and discussions:

Aromatic amino acid Phenylalanine (Phe) derivative Fmoc-Phe-DCU (M1), forms gel in various organic solvents like benzene, chlorobenzene, 1,2 dichlorobenzene (1,2 DCB), tetrahydrofuran (THF), toluene, chloroform, dichloromethane (DCM) and 3-xylene upon being heated and subsequently cooled (Minimum gelation concentration, MGC = 0.2-0.4 %, w/v) (Table1, Figure 1). The gelation properties of M1 are documented in Table 1. M1 contains aromatic side chains of the amino acid residue Phe and an aromatic N terminal protecting group Fluorenylmethyloxycarbonyl (Fmoc). To investigate which if aromatic interactions between any of these groups were involved in gelation, we replaced the Phe residue with two other amino acid residues, a) aromatic Phenylglycine (Phg) to form Fmoc-Phg-DCU (M2) and b) non aromatic gamma aminoisobutyric acid (Gaba) to generate Fmoc-Gaba-DCU (M3). Both M2 and M3 formed gels like M1 and their gelation properties were same as that of M1 (Table 1, Figure 1). This observation indicates that the aromatic side chain of the amino acid residue might not be a necessary factor in the gelation process. The aromatic moiety Fmoc most probably plays an important role in the gelation process. To investigate the role of Fmoc group in the gelation process we designed the control molecule Boc-Gaba-DCU (M4). This molecule did not form gel under the experimental conditions (Figure 1b) suggesting that the π-π stacking of the Fmoc moieties is one of the main drivers for the gelation process. Minimum gelation concentration of most gels for the three gelators in different solvents lies within 0.2 to 0.45 (w/v %) (Table 1). All the molecules M1-M3 have a very low MGC in 1,2 DCB. Moreover, the gels formed from 1,2 DCB were translucent and remained stable for a very long time. Thus

View Article Online
DOI: 10.1039/C9OB00014C

most of the experiments to study the morphology of the organogels have been done in 1, 2 DCB.

The thermal stability of the gel has been studied in different organic solvents by monitoring the gel melting temperature (T_{gel}) at the minimum gelation concentration. The experiment was performed by heating organogels in a thermostatic oil bath with an increment of temperature of 1°C/min until the organogels melted to sol. The T_{gel} values of the gels formed from various solvents have been found to be ranging from 32° to 96° C (Table 1).

The gels formed by M1-M3 are of thermo reversible nature, *i.e*. the gel is reversibly converted into sol upon heating. On cooling the sol, gel is formed once again (Figure 1c). M1 –M3 act as phase selective gelators which can selectively gel the organic part from a mixture of water-organic solvent as shown in the Figure 1d.

Morphological studies:

Morphological features of the gel formed by M1-M3 in 1,2 DCB at MGC has been studied by Field Emission Scanning Electron Microscopy (FESEM) (Figure 2a-c). M1 forms aggregated morphology which is distinctly different from M2 and M3. M2 adopts a fibre-like morphology while M3 forms nano-tape like morphology. The morphology of M1-M3 in solution at 10 mM concentration in 1,2 DCB is distinctly different from that in the gel state as shown in Figure S1.

Rheological studies:

The mechanical strength and stability of the gel is revealed from the viscoelastic properties, which has been studied using rheology (Figure 2d-f). For rheological studies, the storage modulus (G´) and the loss modulus (G´´) were measured as a function of different parameters, including strain sweep and angular frequency. The gels have been formed from M1, M2 and M3 in 1, 2 DCB at 2.0 % w/v for this study. In strain sweep experiment where the storage modulii (G´) and the loss moduli (G´´) for the three organogels have been plotted as a function

View Article Online
DOI: 10.1039/C9OB00014C

of % strain (0.1-10%) (Figure S2) (Table S3), it was found that G´ was higher than G´´(of the order of 10^4 Pa) till a particular strain (Linear viscoelastic region (LVR), γ = 0.1-0.79% for M1, 0.1-0.795% for M2 and 0.123-0.371% for M3), beyond which the two passed through a crossover point (Table S3) which indicated that the materials no longer stayed in the gel state. Beyond the LVR, the G″ value first increased with the increasing strain till the crossover point, and then decreased, which is a characteristic feature of soft glassy materials.[56] An angular frequency sweep experiment was performed where G′ and G″ were plotted against the angular frequency sweep at a constant strain of 0.1% at 25 °C. For the three organogels, the G′ was found to be dominating over G″ till about 100 rad/s. Also, G′ and G″ were found to be independent of angular frequency, in the region 1-100 rad/s which indicated the formation of stable organogels. The storage modulii of the organogels were of the order of $\geq 10^4$ Pa, in the frequency sweep experiment which indicated a considerable mechanical strength of the three organogels.

Non covalent drivers of self-assembly

The molecules designed have the following features: a) Fmoc moiety at the N terminus, b) DCU moiety at the C terminus and c) an intervening amino acid residue which is hydrophobic in nature. Amino acids Phe and Phg have aromatic side chains. Hence, the organogels formed by these molecules have a high chance of being stabilized by the a) π-π interactions in between the N terminal Fmoc groups and/or the side chains of the aromatic residues, b) intermolecular hydrogen bonding in between the NH and CO of the urea groups and amino acids and c) the vander waals interaction in between the hydrophobic amino acid residues. However formation of organogel by M3 which contains the non-aromatic amino acid residue Gaba indicates that aromatic side chains are not necessary for the gelation process. On the contrary, inability of M4 (Boc-Gaba-DCU) to form organogel under similar experimental conditions is a direct proof

View Article Online
DOI: 10.1039/C9OB00014C

that π-π stacking of the N terminal Fmoc moieties is of immense importance in formation of gels. In order to probe the role of the Fmoc groups in the self-assembly process, we studied the concentration dependent fluorescence emission of the Fmoc group. Concentration dependent Nuclear Magnetic Resonance (NMR) and dimethyl sulfoxide (DMSO) solvent titration were performed to study the role of hydrogen bonding in the gelation process. Fourier Transform Infrared (FTIR) spectrum of powdered and xerogel samples were compared.

Fluorescence studies:

The fluorescence emission spectra for M1-M3 in 1, 2 DCB with varying concentrations is shown in Figure 3a-c. The characteristic fluorescence emission peak for monomeric Fmoc group appeared at around 350 nm at lower concentrations for all the three compounds. With increase in the concentration, the peak at 350 nm is blue shifted to about 346 nm for all the compounds. This was accompanied by quenching of the peak intensity in some of the cases. In an earlier study, such blue shift in the fluorescence emission of ANS was reported upon increasing the hydrophobicity of the microenvironment.[57] In the present context, blue shift of Fmoc emission maxima indicates, increase in the hydrophobicity of the microenviornment around the Fmoc moieties, which might be a consequence of π-π stacking of the Fmoc moieties upon progressive self-assembly. In the fluorescence spectra of M3, upon increasing the concentration, additional broad peaks appear at 415 nm and 450 nm, which might be attributed to the excimer peaks. Absence of side chains in Gaba used in M3, might lead to closer packing of the molecules leading to appearance of excimer peaks. Blue shifting of the emission maxima with increasing concentration, is an indication of the increasing hydrophobic environment, which is a predictable consequence of increasing self-assembly. In brief, the concentration dependent fluorescence emission spectra clearly indicate the presence of π-π stacking among the Fmoc groups upon increasing the concentration. Hence aromatic π-π stacking may be one

of the key factor in driving the gelation process.

View Article Online
DOI: 10.1039/C9OB00014C

FTIR Spectroscopy

Figure S3a-c shows the superimpositions of FTIR of M1-M3 respectively, from the powdered sample and the xerogels obtained from 1,2 DCB. The molecules contain two NH protons and two carbonyl moieties. Peaks for NH protons in molecules M1-M3 in the powdered state appear at 3416/3319 cm^{-1}, 3405/3321 cm^{-1} and 3358/3315 cm^{-1} respectively. These peaks get significantly broadened in the xerogel state for all the compounds. Similarly the Fmoc carbamate carbonyl, the amino acid carbonyl and the urea amide carbonyls which give distinct peaks in the region of 1706-1650 cm^{-1}in the molecules M1-M3 in the powdered state is noticeably diminished in the xerogel state.

NMR Spectroscopy :

The role of intermolecular hydrogen bonds in formation of the self-assembly of the peptides is probed by performing concentration dependent ^1H NMR experiment and monitoring the change in chemical shifts of the NH groups present in the molecules. Figure 4a shows the overlay of the NH regions of the ^1H NMR spectra obtained for M2 at different concentrations (0.125 mM, 0.25 mM, 0.5 mM, 1 mM, 2 mM, 3.44 mM (MGC) and 5 mM) in $CDCl_3$.Concentrations less than MGC, MGC and higher than MGC were selected. There was no visible change in the chemical shifts of the two amide protons of M2 across the entire concentration range (0.125 mM - 5 mM) indicating that there was no change in the electron density about the amide protons or in other words there was no change in the hydrogen bonding status of the two amides in this concentration range. To find out the hydrogen bonding status of the amide protons, we performed a DMSO titration experiment (Figure 4b). M2 was dissolved in a non-polar and inert solvent $CDCl_3$ and an NMR was recorded initially. $CDCl_3$ being non polar was incapable of forming hydrogen bonds with the amide protons of M2. To

View Article Online
DOI: 10.1039/C9OB00014C

this, increasing amounts of polar solvent DMSO-d_6 was added, which formed hydrogen bonds with the non-hydrogen bonded amide protons of M2 leading to a downfield shift of the concerned signals in the NMR. Signals of amide protons which were already intra or intermolecularly (solute-solute) hydrogen bonded in $CDCl_3$ did not show any change in the chemical shifts. Amide proton of urea (N-H_a) did not show any change in its chemical shift while the amide proton of the amino acid Phg (N-H_b) showed a considerable downfield shift ($\Delta\delta$ =0.85 ppm) indicating that the N-H_a was hydrogen bonded unlike the Phg amide proton in non polar solvent like $CDCl_3$.

Powder X-ray Diffraction (PXRD)

PXRD studies have been carried out to obtain information about molecular packing of M1-M3 in gel state. PXRD pattern of the xerogels obtained from 1,2 DCB in the wide angle regions for M1-M3 is shown in Figure S3d-f. The wide angle PXRD patterns of all the xerogels show periodic diffraction patterns unlike the powdered samples and this indicates presence of ordered structures in their xerogel form. PXRD pattern for xerogels of all the three molecules M1-M3 looks identical suggesting that very similar packing pattern is present in all of them. The peak at 2θ = 21.88° (d = 4.08 Å), 21.78° (d = 4.08 Å) and 21.9° (d = 4.06 Å) for M1-M3 might correspond to the π-π stacking distance in between the aromatic moieties of the gelator molecules.[16] The peak at 2θ =18.56° (d = 4.78 Å), 18.90° (d = 4.69 Å) and 18.94° (d = 4.68 Å) for M1-M3 might correspond to the distance in between the C-terminal ends of the gelator molecules.[16]

Dye absorption studies:

The organogels formed by the molecules M1-M3 were subjected to the dye absorption studies with the aim to employ these organogels for purifying water contaminated with toxic dyes. We checked the dye absorption by the gels with three dyes, namely crystal violet (CV), neutral red (NR) and rhodamine B (RB). When the mixture of the organic solution of LMWG and aqueous

solution of dye was heated and subsequently cooled, the organic phase with the LMWG molecule selectively formed gel and absorbed the dye from the aqueous solution within some time. This was studied by monitoring UV of the aqueous phase (Figure 5a-c, S4) along with the visible fading of the color of the aqueous phase as shown in the figure S5. All the organogels acted as very efficient dye absorbents with about 90% efficiency for all the dyes (Figure 5d, Table S2).

Reusability of the gel: In order to be efficiently used as a material for water purification, the material should be economic and hence, recyclable. The organogels from M1-M3 could be reused over three cycles for subsequent loading and release of the dye, after which the quality of the dye degraded (Figure S6). Figure 6a shows the percentage efficiency of CV uptake in 24 hours in the three subsequent cycles and Figure 6b indicates percentage release of CV after 16 hours in the three subsequent cycles from M1 organogel. Figure 6c compares the diminishing loading and release efficiencies of M1 organogel in the three subsequent cycles.

Ion sensing studies: As our molecules contain urea moiety which is known widely as a fluoride ion sensor, we looked into anion sensing abilities of M1-M3. We first decided to look at the UV-Vis absorption and fluorescence behavior of M1-M3 in the absence and the presence of various anions like fluoride, chloride, bromide, iodide, bisulphate, phosphate, acetate and hydroxide (as their Bu_4N^+salts) (Figure 7, S7, S8). The spectroscopic studies were performed in acetonitrile (ACN) as the molecules did not form gel in this solvent. Secondly, ACN was inert and did not have any absorption in the range 200-600 nm. UV absorption of M1-M3 was only sensitive to fluoride, acetate and hydroxide (Figure 7a, S7a, S8a). In the absence of anions, M2 (Figure 8a) and M1 (Figure S7a) contained peaks at 265 nm, 289 nm and 299 nm. Shoulders were observed at 255 nm and 272 nm. Upon addition of fluoride, acetate and hydroxide, the shoulder at 255 nm developed into a peak with appearance of another new peak at 245 nm. The peak at 289 nm disappeared. Peaks at 265 and 299 nm remained unchanged (Figure 8a-c).In

View Article Online
DOI: 10.1039/C9OB00014C

the presence of other anions (Cl^-, Br^-, I^-, HSO_4^-, PO_4^-), there was no change in peak positions and minor changes in peak intensities (Figure 7a, S7a). M3 had similar UV absorptions as M1 and M2, which did not change appreciably upon addition of any anions (Figure S8a).

In order to look at the effect of the anions on the excited state of the molecules, change of the fluorescence signal in the presence of anions was studied (Figure 7b, S7b, S8b). In the absence of anions, upon being excited at 301 nm, the fluorescence emission maxima for M1-M3 was at 332 nm. Upon addition of 0.1mM fluoride, acetate and hydroxide, the peak at 332 nm was slightly blue shifted (for M1 and M3) (Figure S7b, S8b) and quenched (predominantly for M2) (Figure 7b). A prominent new peak appeared at 459 nm for all the three molecules M1-M3. There was negligible effect on the fluorescence spectra of M1-M3 in the presence of other ions (Figure 7b, S7b and S8b). Thus it was concluded that molecules M1-M3 selectively sensed fluoride, acetate and hydroxide anions. To find out the sensitivity of anion detection, the fluorescence response was monitored as a function of anion concentration for a fixed concentration of M1-M3 (Figure 8d-f, S9-13b). For all the three molecules, anions could be detected at a minimum concentration level of about 0.02 mM. With increase in the concentration of the anion, the intensity of the peak at 459 nm steadily increased.

In order to understand the interaction in between fluoride anion and M1-M3 in greater detail, ^{1}H NMR titration experiment was carried out with M2 in the presence of fluoride ions (Figure 9). With increasing concentration of F^-, the urea NH (N-H_a) shows no change in its chemical shift value while the NH proton of the amino acid Phg (N-H_b) disappears quickly with a downfield shift ($\Delta\delta$ = 0.24 ppm). This observation indicates that strong interaction via hydrogen bonds exists between the amino acid NH (N-H_b) and the fluoride in the anion complexed form. The urea NH does not seem to form any hydrogen bonds with the anions as it is already intramolecularly hydrogen bonded as seen from the DMSO titration of M2 (Figure 4b).

View Article Online
DOI: 10.1039/C9OB00014C

To study the effect of the anions on the ability of formation and the disruption (gel-sol transition) of organogels, the anions were added a) to the organic solvent containing M1-M3, heated together and cooled subsequently(Figure S14a-c, S15a-c, S16a-c) and b) to the preformed gel (Figure 14d-f, 15d-f, 16d-f). This study was performed only with those anions which had a fluorescence response. Fluoride prevented gel formation in all of the LMWG molecules, while hydroxide prevented gel formation only in M2 and M3. Gel formation was not prevented by acetate for any of the molecules M1-M3. None of the anions could disrupt preformed gels formed by M1 to M3 (FigureS14d-f, S15d-f, S16d-f).The varying response towards the anions might be associated with the varying strength of self-assembly of different gels.

Electronic structure calculations

We performed DFT studies for understanding the mode of binding of fluoride to the M2 molecule at the atomic level. The optimized ground state structures of M2 monomer and its fluoride bound M2:F^- complex are shown in Figure 10. N-H_a (DCU) and N-H_b (amino acid backbone) bond lengths are almost identical, former being slightly elongated for free M2 monomer (Figure 10a). Intramolecular hydrogen bond between N-H_a of DCU and carbonyl of amino acid backbone in the six-membered ring is a characteristic feature of M2. The angle N-H_a…O is 132.5° and H_a…O distance is 1.81Å respectively. This feature is supported by the ^{1}H NMR DMSO titration experiment discussed earlier (Figure 4b) in which N-H_a was shown to be intramolecularly hydrogen bonded. Calculations suggest two possible fluoride binding modes which are isoenergetic; single (M2:F^-_S1, Figure 10b) and double (M2:F^-_S2, Figure 10c) intermolecular hydrogen bonds between F^- and M2. This suggests that the double hydrogen bonded interaction between M2 and F^- is offset by disruption of favorable intramolecular hydrogen bonding between N-H_a and CO of amino acid. In M2:F^-_S1 fluoride

View Article Online
DOI: 10.1039/C9OB00014C

binding to the amino acid backbone N-H_b leads to elongation of the N-H_b bond length from 1.01Å to 1.09Å (Figure 10b). F^-…H_b distance is 1.43Å and the orientation of the six-membered ring relative to N-H_b is altered upon fluoride binding (Figure 10b).. N-H_b, F-…H_b distances in the double hydrogen bonded M2:F^-_S2 are 1.06Å and 1.51-1.54Å respectively. The shorter F^-…H_b and larger N-H_b in M2:F^-_S1 with respect to M2:F^-_S2 makes N-H_b of the former more susceptible towards fluoride induced deprotonation. This observation is in lines with the ^{1}H NMR titration experiment discussed above (Figure 9). However, fully deprotonated form ($M2^-$:HF) was not observed upon geometry optimization starting with different geometries with varying F^-…H_b and N-H_b distances in single intermolecular binding mode. Optimization with different initial geometries always gave M2:F^-_S1 (Figure 10b). Calculated normal model frequencies of all the optimized geometries indicate that all the reported structures were true minima on the potential energy hyper surface. The optimized geometries of M2:X^- (X = Cl, Br, I, OH, OAc) are given in the supporting information (Figure S17). The calculated absorption spectra of M2 and M2:$F^-$are shown in Figure 10c and calculated absorption peaks are listed in Table 2. For M2 monomer, the first calculated absorption peak located at 265.64nm, is in excellent agreement with the experiment (Figure 7a). This absorption is primarily assigned to the highest occupied molecular orbital (HOMO) to lowest unoccupied molecular orbital (LUMO) transition (Figure 7a). Characteristic absorption peaks of fluoride bound M2:F^- at 255 nm and 246 nm were also reproduced by theoretical calculations (Table 2). The molecular orbitals relevant to the absorption peaks are shown in Figure S18.

Having understood now that the urea NH (N-H_a) is actually not involved in the fluoride binding event we asked the question if the DCU moiety is important at all in the ion sensing abilities of M1-M3. To probe this we considered the control molecule Fmoc-Phe-OH and studied its ion sensing abilities. There is no UV absorption or fluorescence response in the presence of any of the anions that were tested (Figure S19). This is a crucial evidence which indicates that

View Article Online
DOI: 10.1039/C9OB00014C

the DCU moiety of the M1-M3 plays a significant role in their ion sensing. This might be due to the role of DCU moiety in modulating the molecular orbitals in a specific manner that leads to fluorescence response in the ion detection.

Self-Assembly mechanism and the anion sensing

Figure S20 summarizes the mechanism of self-assembly of M1-M3. From all the studies above it can be concluded that π-π stacking of the Fmoc moieties and the hydrophobic effect are the two most important forces driving the self-assembly of M1-M3. Hydrogen bonding seems trivial in this process.

Involvement of the urea NH (N-H_a) in intra molecular hydrogen bond, forming the six membered ring is supported by the NMR experiments and DFT studies (Figure 4b and 10a). The backbone N-H_b of Phg is non-hydrogen bonded (Figure 4b) and remains so in the hydrophobic pockets even at concentrations greater than MGC indicating that intermolecular hydrogen bonds are not the driving forces for the self-assembly process. In the self-assembled state, adjacent molecules come close and the Fmoc groups are stacked together at 180 degrees to each other. This is supported by the PXRD data where the interplaner distance of about 4.07 ± 0.1 Å is obtained which is the ideal distance for aromatic stacking. However stacking of the Fmoc moieties most probably occurs by approach of adjacent molecules from opposite sides (Figure S18).This happens firstly as the C terminal end of the amino acid residue contains dicyclohexyl urea moieties which impart non-planarity to the molecules, preventing adjacent molecules to approach as close as 4Å from the same side. Secondly, side chains of Phe and Phg contain bulky Ph groups, in a plane which is almost perpendicular to that of the Fmoc moieties. This also prevents same side approach of molecules (Figure 9a). In an alternate possibility, the adjacent molecules may approach each other orthogonally or at different other angles, for Fmoc stacking. These different modes of assembly may account for the different gel state morphology obtained for M1-M3 starting from aggregated-like to fibre-like to

View Article Online
DOI: 10.1039/C9OB00014C

flattened nano-tapes (Figure 2a-c). In M3, amino acid Gaba does not contain any side chains, which leads to better stacking of the molecules than in M1 and M2. This is supported by the presence of excimer peaks only in the fluorescence spectra of M3 (Figure 3c).

Among the different anions screened, only F^-, OAc^- and OH^- are specifically sensed, as these are the strongest bases among all and hence have the greatest tendency to bind the acidic N-H_b of M1-M3. As the NH of urea (N-H_a) is intramolecularly hydrogen bonded, the only NH available for the anion complexation is the N-H_b from the amino acid. Upon complexation with the anion, the backbone of the molecule gets distorted as seen from the DFT studies. This in turn prevents the approach of the molecules close enough to let -π-π aromatic stacking possible and thus prevents gelation process. This explains the inability of M1-M3 to form gels in the presence of anions. Once the gelation occurs, the non-hydrogen bonded N-H_b that complexes with the anions is housed deep in the hydrophobic pocket. This pocket is flanked by the Fmoc stacking on one side and the non-planer DCU moiety on the other. Moreover, fluoride and other anions being highly charged does not prefer to enter into the hydrophobic pocket to access the non- hydrogen bonded NH. This explains why the anions have no effect on the organogels.

Experimental Section:

Materials and methods:

L-Phe, L-Phg, Gaba , N, N′ – dicyclohexyl urea and all other organic solvents used in gelation were purchased from Spectrochem. Fmoc-OSu was purchased from G. L. Biochem Ltd.

Amino acid based DCU derivatives were synthesized by solution phase methodology. The N-termini of the amino acids were protected by Fmoc group using Fmoc-OSu while the C-termini were protected by dicyclohexylcarbodimide (DCC). All the compounds were purified using column chromatography using silica gel (100-200 mesh size) as stationary phase and hexane and ethyl acetate as eluent. Finally, compounds were characterized by analytical HPLC, ^{1}H NMR (400MHz), and mass spectrometry.

View Article Online
DOI: 10.1039/C9OB00014C

General procedure for synthesis:

Synthesis of Fmoc-protected amino acids: The amino acid (5mmol, 1eq) (L-Phe, L-Phg and Gaba) was dissolved in water and sodium bicarbonate (10 mmol, 2 eq) was added with stirring. The resulting solution was cooled to 5°C and Fmoc-OSu (7.5 mmol, 1.5 eq) was added slowly as a solution in 1, 4-dioxane (also cooled). The resulting mixture was stirred at 0 °C for 1 hour and allowed to warm to room temperature overnight. Dioxane was evaporated and water was added to the residue. The aqueous layer was extracted three times with ethyl acetate. The aqueous layer was then acidified to pH 1 with 10% HCl and extracted three times with ethyl acetate. The combined organic layers were dried over sodium sulphate and concentrated *in vacuo* to obtain the product (Fmoc-AA-OH) which was then purified by column chromatography using hexane and ethyl acetate as the eluent.

Yield: Fmoc-Gaba-OH, 4.32 mmol, 86.4%; Fmoc- Phe-OH, 3.98 mmol , 79.6% and Fmoc-Phg-OH, 4.10 mmol, 82% .

Synthesis of Fmoc-AA-dicyclohexylurea carbamate: To a solution of Fmoc-AA-OH, (1 eq) in DCM (15 ml), DCC, 2 eq. was added and the mixture was stirred for 48 h at room temperature. 50 ml of ethyl acetate was added to the reaction mixture and dicyclohexylurea (DCU) was filtered off. The organic layer was washed three times with 1 M sodium carbonate (50 ml) and two times with brine (50 ml), dried over anhydrous sodium sulfate and evaporated *in vacuo* followed by purification using column chromatography to obtain a solid product.

Yield: M1: 2.10 mmol, 52.7 %; M2, 2.97 mmol, 72.5% and M3: 2.75 mmol, 63.6%.

M1-M4 were characterized using analytical HPLC (Figure S21-S24), ESI-HRMS (Figure S25-S28), ^{1}H NMR (S29-S32) and ^{13}C NMR (S33-S36).

M1(Figure S29): ^{1}H NMR (400 MHz, $CDCl_3$) δ 7.73 (d, **2H**, aromatic ring Hs), 7.50 (dt, **2H**, aromatic ring Hs), 7.39 – 7.24 (m, **7H**, aromatic ring Hs), 7.19 – 7.14 (m, **2H**, aromatic ring Hs), 5.37 (d,**1H**, N<u>H</u>-CH), 4.68 (m, **1H**, N<u>H</u>-CH,cyclohexyl), 4.27(d, **2H**, -C<u>H</u>$_2$-CH- of Fmoc-

View Article Online
DOI: 10.1039/C9OB00014C

), 4.18– 4.02 (m, **2H**, -CH_2-C<u>H</u>- of Fmoc and –C<u>H</u>-, alpha H of Phe),), 3.67– 3.54(m, **1H**, cyclohexyl C<u>H</u>-NH), 3.11-2.82(ddd, **2H**, C<u>H_2</u>, beta H of Phe), 1.93-1.02 (m, **21**H, cyclohexyl Hs).

M1(Figure S33): ^{13}C NMR (101 MHz, $CDCl_3$) δ 156.42, 152.85, 143.77, 143.61, 141.27, 136.03, 129.25, 128.76, 127.74, 127.24, 127.09, 127.05, 125.14, 120.00, 77.34, 77.03, 76.71, 67.36, 54.85, 47.01, 39.11, 32.51, 31.94, 31.32, 29.72, 26.00, 25.93, 25.37, 25.30, 24.71, 0.00.

M2 (Figure S30): ^{1}H NMR (400 MHz, $CDCl_3$) δ 7.72(d, **2H**, aromatic ring Hs), 7.58 – 7.52 (m, **2H**, aromatic ring Hs), 7.41-7.257.39 (m, **9H**, aromatic ring Hs), , 5.88 (d, **1H**, N<u>H</u>-CH), 5.63 (d, **1H**, N<u>H</u>-CH,cyclohexyl), 4.40 – 4.28 (m, **2H**, -C<u>H_2</u>-CH- of Fmoc-), 4.18(t, **1H**, -CH_2-C<u>H</u>- of Fmoc), 4.00 (s broad, , **1H**, -C<u>H</u>-NH, alpha H of Phg), 3.64 (dtd, **1H**, cyclohexyl C<u>H</u>-NH), 2.00-1.04 (m, **21**H, cyclohexyl Hs).

M2 (Figure S34): ^{13}C NMR (101 MHz, $CDCl_3$) δ 156.11, 153.08, 143.87, 143.60, 141.29, 129.17, 128.86, 127.75, 127.59, 127.09, 125.18, 125.10, 120.00, 77.34, 77.02, 76.70, 67.41, 57.75, 50.21, 47.08, 32.55, 32.25, 31.18, 29.59, 26.04, 25.43, 25.24, 24.68, 0.00.

M3(Figure S31): ^{1}H NMR (600 MHz, $CDCl_3$) δ 7.77 (d, **2H**, aromatic ring Hs of Fmoc-), 7.59 (d, **2H**, aromatic ring Hs of Fmoc-), 7.40 (t, **2H**, aromatic ring Hs of Fmoc-), 7.32 (td, **2H**, aromatic ring Hs of Fmoc-), 5.16 (s, **1H**, N<u>H</u>-CH_2), 4.33 (d, **2H**, -C<u>H_2</u>-CH- of Fmoc-), 4.20 (t, **1H**, -CH_2-C<u>H</u>- of Fmoc), 3.96 (s, **1H**, N<u>H</u>-CH, cyclohexyl), 3.72 – 3.63 (m, **1H**, cyclohexyl C<u>H</u>-NH), 3.28 (m, **2H**, -C<u>H_2</u>-CH_2-CH_2-CO), 3.15 (m, **2H**, -C<u>H_2</u>-CH_2-CO), 2.48 (t, **2H**, -CH_2-C<u>H_2</u>-CO), 1.96-1.05 (m, **21**H, cyclohexyl Hs);

M3 (Figure S35): ^{13}C NMR (101 MHz, $CDCl_3$) δ 143.93, 141.31, 127.73, 127.09, 125.10, 119.99, 77.33, 77.02, 76.70, 32.64, 30.95, 26.08, 25.51, 24.71, -0.00.

M4(Figure S32): ^{1}H NMR (400 MHz, $CDCl_3$) δ 1.42 {s, **9H**, -$(CH_3)_2$ of Boc group}, 6.86 (s, **1H**, N<u>H</u>-CH), 4.72(s, **1H**, N<u>H</u>-CH,cyclohexyl), 3.93 (m, **2H**, -C<u>H_2</u>-CH_2-CH_2-CO), 3.71 – 3.64

(m, **1H**, cyclohexyl C<u>H</u>-NH), 3.17 (m, **2H**, -C<u>H</u>$_2$-CH$_2$-CO), 2.44 (t, **2H**, -CH$_2$-C<u>H</u>$_2$-CO), 2.00 – 1.04 (m, **21**H, cyclohexyl Hs)

M4 (Figure S36): ^{13}C NMR (101 MHz, $CDCl_3$) δ 156.21, 154.08, 77.33, 77.01, 76.69, 49.95, 32.84, 32.68, 30.91, 28.43, 26.23, 25.61, 25.47, 25.35, 24.74, -0.01.

Gelation experiments:

To check the ability of the gelator molecules to form gel in different solvents, weighed amount of the synthesized compounds (M1-M3) were taken in vials and 500 µL of different solvents were added to them. Samples were heated in a heating block at temperatures ranging from 60 °C- 100 °C and subsequently cooled to room temperature. Gel was formed within 15 minutes which was stable to inversion of the glass vials.

Determination of the gel-to-sol transition temperature:

The gel-to-sol transition temperature (T_{gel}) was determined by placing the gel containing vial in an oil bath and slowly raising the temperature of the bath at the rate of 1°C per minute. The temperature was monitored using a thermometer. The (T_{gel}) was defined as the temperature at which the gel melted and started to flow.

Rheology:

The viscoelastic properties of organogels were determined by rheology studies using Anton Paar MCR102 Rheometer equipped with a 20 mm parallel-plate measuring system at 25 °C at a concentration of 2.0 w/v% in 1, 2 DCB. A strain sweep test was performed over a range from 0.1-10% strain at a fixed oscillatory frequency of 1 rad/s. Furthermore the mechanical strength of the organogels were determined from the oscillatory test, ie. frequency sweep, which was carried out under an appropriate strain of 0.1% with the frequency ranging from 1-100. Rheological experiments measure two parameters; storage modulus (G′) and loss modulus

View Article Online
DOI: 10.1039/C9OB00014C

(G″). A defining measure of gelation process is having a higher value of G′ than G″ which are essentially independent of frequency.

FESEM :

FESEM images of the reported materials M1-M3 were obtained on a FESEM Sigma Zeiss Gemini microscope. A drop of the solution of the gelator molecules in 1,2-DCB was casted on a silicon wafer and was allowed to dry for a few hours under vacuum before imaging. For the morphology of the organogel, it was casted on the silicon wafer and allowed to dry under vacuum before imaging.

Fluorescence spectroscopy:

To gain an insight into the self-assembly behavior of M1-M3, fluorescence experiments were performed by monitoring the fluorescence of the Fmoc moiety on a Fluoromax-4 spectrophotometer. Samples of different concentrations were prepared in 1,2-DCB and their fluorescence emission was monitored keeping the fluorescence excitation wavelength fixed at 301 nm.

FTIR :

FT-IR spectroscopy measurements were recorded on a Spectrum Two Perkin Elmer FT-IR Instrument using KBr pellets. Measurements were performed on powdered samples and on the xerogel obtained for M1-M3 and the two were compared with each other.

NMR experiments:

NMR experiments were performed on a 400 MHz Bruker NMR spectrometer. ^{1}H NMR experiments were performed for routine characterization of the molecule. Concentration dependent ^{1}H NMR (0.25 mM, 0.5 mM, 1 mM, 2 mM, 3.44 mM (MGC) and 5 mM) was recorded for the molecule M2 in $CDCl_3$ at ambient temperature. DMSO titration was performed at 5mM concentration of M2 and 0.5% to 15% DMSO concentrations in $CDCl_3$ at ambient temperature. ^{1}H NMR experiments were conducted at different concentrations of fluoride ions

View Article Online
DOI: 10.1039/C9OB00014C

to understand the mode of interaction between the molecules and fluoride ions for its anion sensing functions.

PXRD:

Wide angle X-ray diffraction analysis was done on a Bruker D2 Phaser X Ray diffractometer (Cu-Kα radiation, χ=1.5406 Å) for both the powdered samples and the xerogels obtained from drying the organogels of M1-M3 obtained from 1,2 DCB.

Dye absorption studies

2 mg of the gelator molecule was dissolved in 500 µL of 1,2 DCB. Into it the aqueous solution of dye (500 µL) was added and the mixture was heated at 100 ˚C for 10 minutes. Upon cooling the mixture, the bottom layer i.e. the organic solvent 1, 2-DCB with the gelator formed the gel while the aqueous phase formed a supernatant over the gel. This was allowed to stand for 24 hours at RT, after which the amount of unabsorbed dye in the supernatant was checked by monitoring the UV of the supernatant aqueous solution and calculating the concentration from a standard curve of the dye. The amount of dye loaded in the gel and the dye loading efficiency were then calculated as follows:

Dye loaded = (Initial dye-Unabsorbed dye)

Loading efficiency: Dye loaded/Initial dye X 100

Recycling of the gel in dye absorption/release:

CV dye loading was in each cycle was calculated as described above. To the dye loaded gel, 500 µL of diethyl ether was added as the release medium. Diethyl ether layer was then taken out after 1 hr and kept in a vial (V1), 500 µL of fresh ether was added to the gel for release which was subsequently taken out after 3 hrs (V2). This was repeated for another three times at time gaps of 6, 10 and 16 hours (V3, V4 and V5 respectively). Each time the diethyl ether where the dye was released was taken out and kept in vials (V1-V5) for evaporation. After

View Article Online
DOI: 10.1039/C9OB00014C

complete evaporation of ether, 500 µL of water was added to V1 and its absorbance was monitored. Then the contents of V1 were added to V2 for monitoring the UV. In this way the contents of each vial was added to the next one for UV monitoring at time intervals of 1,3, 6,10 and 16 hours. From the UV data, amount of dye released at these different time points could be easily calculated using a standard curve for the dye. Percentage of the amount of dye released in cycle 1 was calculated with respect to the dye loaded.

Dye release efficiency was calculated as follows:

Release Efficiency: Dye released in a cycle/ Dye loaded in the cycle X 100

For the second cycle, 500 µL, 40µM dye solution was added to the gel again for dye loading studies. The rest of the experiment was done as already described above. Amount of dye loaded and released in each cycle was calculated. The gel could be reused effectively for three cycles after which the quality of the gel degraded.

Anion sensing:

A stock solution of 1 mM of the gelator molecules in ACN was prepared. Stock solutions of 10 mM tetrabutylammonium salts of F^-, Cl^-, Br^-, I^-, H_2PO_4, OH^-, ACO^- and HSO_4^- were prepared in ACN. Then a solution of 0.2 mM of the gelator molecules were prepared from the stock solution. Also, 0.2 mM of all the anion solutions were prepared from the 10 mM stock solution. For monitoring UV and fluorescence spectra 500 µL of 0.2 mM of the gelator solution was taken and into it 500 µL of 0.2 mM anion solution was added so that the final concentration of the gelator and the anion solution became 0.1 mM. The UV and fluorescence was monitored for all the anions with the three gelators. Anion sensing was studied with Fmoc-Phe-OH as control. For monitoring UV and fluorescence spectra 500 µL of 0.2 mM of the solution of Fmoc-Phe-OH was taken and into it 500 µL of 0.2 mM anion solution was added so that the final concentration of the molecule and the anion in solution became 0.1mM.

View Article Online
DOI: 10.1039/C9OB00014C

Titration of the gelator molecules with specific anions:

500 µL of 0.2 mM of gelator solution in ACN was taken in different 1 ml volumetric flasks and into it 500 µL of different concentration of the anion solution were added so that the final concentration of the gelator solution becomes 0.1 mM. The UV and the fluorescence of these solutions were then monitored as described above. UV was monitored using a wavelength scan for 200-700 nm. The fluorescence emission was monitored for excitation wavelength of 301 nm.

Computational Details

DFT/TDDFT calculations were performed by the Gaussian 09 program package[58] using **6-31+G*** basis set. Geometry optimizations of dicyclohexyl urea derivative (M2) in its free and anion bound state was performed without symmetry constraints. Normal mode analysis has been performed for ensuring true local minimum geometry. Polarizable continuum model (PCM)[59] with ACN as solvent was used to include the solvent effects in all the calculations. A dielectric constant (ε) of 36.64 ACN was used for including solvent effect. Gas-phase optimized geometries were subjected to further optimization in ACN solvent. Based on optimized geometries of the ground states, the absorption spectra of free M2, and its complexes M2:X^- (X@F, Cl, Br, I, AcO, OH) were calculated by the TDDFT methods, at the same level of theory. Several possible geometries of free M2 and anion bound M2:X^- was studied.

Conclusions:

In our present study we have reported a new class of LMWG. Dicyclohexyl urea derivatives of amino acids are extremely simple molecules that easily form organogels in a large range of organic solvents. The mechanism of gelation has been analyzed in detail and it has been proved that molecular self-assembly is driven by π-π interaction in between the Fmoc moieties and

hydrophobic effect. The reported organogels are capable of absorbing different organic dyes highly efficiently and are recyclable in nature. M1-M3 can act as selective anion sensors for fluoride, hydroxide and acetate. The mechanism of fluoride sensing has been clearly understood and the mode of fluoride binding established both by experimental and computational methods. We may conclude by saying that this new class of amino acid derivatives of urea forms easily synthesizable and cost effective materials which can have multiple applications like water purification by removal of toxic dyes effectively and as anion sensors for selective anions like fluoride, acetate and hydroxide.

Author contributions:

SC designed the project, KR performed most of the experiments, MC performed PXRD, FTIR and dye absorption experiments, SG did the electronic structure calculations. SC and PS analyzed the data and wrote the paper.

Acknowledgements:

SC would like to acknowledge Department of Science and Technology, India (Fast Track Project No: SB/FT/CS-070/2014) for the financial support required for this research. KR, MC and SG acknowledge IIT Guwahati for Scholarship, and Central Instruments Facility, IITG for the FESEM instrument facility. SC acknowledges Nilotpal Singha for performing the Rheology experiment and Dr. D. Das for insightful discussions. Computing facility by Biomolecular Simulation Lab (BSL, BSBE department, IIT Guwahati) and BIF, IIT Guwahati, Central Instrument facility IIT Guwahati is gratefully acknowledged.

References:

1. P. Terech and R. G. Weiss, *Chem. Rev*., 1997, **97**, 3133.
2. E. R. Draper and D. J. Adams, *Chem* , 2017, **3,** 390.

View Article Online
DOI: 10.1039/C9OB00014C

3. N. M. Sangeetha and U. Maitra, *Chem. Soc. Rev*., 2005, **34**, 821.
4. P. Anilkumar and M. Jayakannan, *J. Phys. Chem. B*, 2010, 114, 728.
5. A. Ajayaghosh and V. K. Praveen, *Acc. Chem. Res*., 2007, **40**, 644.
6. A. Shumburo and M. C. Biewer, *Chem. Mater*., 2002, **14**, 3745.
7. S. Bhattacharya and S. K. Samanta, *Chem.Rev*., 2016, **116**, 11967.
8. W. Kubo, T. Kitamura, K. Hanabusa, Y. Wada and S. Yanagida, *Chem. Commun*., 2002, 374.
9. E. A. Wilder, K. S. Wilson, J. B. Quinn, D. Skrtic and J. M. Antonucci, *Chem. Mater*., 2005,**17**, 2946.
10. C. L. Esposito, P. Kirilov and V. G. Roullin, *J. Control Release*, 2018, **271**, 1.
11. W. Liyanage, K. Vats, A. Rajbhandary, D. S. W. Benoit and B. L. Nilsson, *Chem. Commun*., 2015, **51**, 11260
12. L. Szkolar, J.-B. Guilbaud, A. F. Miller, J. E. Gough and A. Saiani, *J. Pept. Sci*., 2014, **20**, 578.
13. K. Basu, N. Nandi, B. Mondal, A. Dehsorkhi, I. W. Hamley and A. Bannerjee, *Interface Focus*, 2017,**7**,1
14. M. Konda, I. Maity, D. B. Rasaleand A. K. Das, *ChemPlusChem*, 2014, **79**, 1482.
15. X. Zhang, J. Song, W. Ji, N. Xu, N. Gao, X. Zhang and H. Yu, *J. Mater. Chem. A*, 2015,**3**, 18953.
16. S. Basak, J. Nanda and A. Banerjee, *J. Mater. Chem*., 2012, **22**, 11658.
17. B. O. Okesola and D. K. Smith, *Chem. Soc. Rev*., 2016**, 45,** 4226.
18. S. Panja, S. Bhattacharya and K. Ghosh, *Langmuir*, 2017, **33**, 8277.
19. S. Marullo, C. Rizzo, N. T. Dintcheva, F. Gianicci, F. D' Anna, *J. Coll. Interface Sci.*, 2018, **517**, 182.
20. N. Cheng, Q. Hu, Y. Guo, Y. Wang, L. Yu, *ACS Appl. Mater. Interfaces*, 2015, **7**, 10258.

21. C. Rizzo, S. Marullo, P. R. Campodonico, I. Pibiri N. T. Dintcheva, R. Noto, D. Millan, F. D'Anna *ACS Sustainable Chem. Eng*. 2018, **6**, 12453.

22. C. Rizzo, R. Arrigo, N. T. Dintcheva, G. Gallo, F. Gianicci, R. Noto, A. Sutera, p. Vitale, F. D'Anna, *Chem. Eur. J*., 2017, **23**, 16297.

23. B. Adhikari, J. Nanda and A. Banerjee, *Chem.Eur. J*., 2011, **17**, 11488.

24. C. Giansante, G. Raffy, C. Schafer, H. Rahma, M.-T. Kao, A. G. L. Olive and A. D. Guerzo, *J. Am. Chem. Soc*., 2011, **133**, 316.

25. N. Mohmeyer and H. W. Schmidt, *Chem. Eur. J*., 2005, **11,** 863

26. M. Suzuki, T. Nigawara, M. Yumoto, M. Kimura, H. Shirai and K. Hanabusa, *Org. Biomol. Chem*., 2003, **1**, 4124.

27. M. Suzuki, Y. Nakajima, M. Yumoto, M. Kimura, H. Shirai and K. Hanabusa, *Org. Biomol. Chem.* 2004, **2**, 1155.

28. G. Wang and A. D. Hamilton, *Angew. Chem. Int. Ed*., 2000, **112,** 2263.

29. M. Suzuki, Y. Sakakibara, S. Kobayashi, M. Kimura, H. Shirai and K. Hanabusa, *Polym. J*., 2002, **34**, 474.

30. F. Placin, J.-P. Desvergne and J.-C. Lassegues, *Chem. Mater*., 2001, **13**, 117.

31. N. Basu, A. Chakraborty and R. Ghosh, *Gels*, 2018, **52**, 1.

32. S. S. Babu, V.K.Praveen and A. Ajayghosh, *Chem. Rev.*, 2014, **114**, 2129.

33. B. Gioia, N. B. Ghalia and P. Kirilov, *Journal of Pharmacy and Pharmaceutical Science*, 2018, **7**, 1.

34. S. Samai, J. Dey and K. Biradha, *Soft Matter*, 2011, **7**, 2121.

35. I.A. Coates, A.R. Hirst and D. K. Smith, *J. Org. Chem*., 2007, **72**, 3937.

36. V. Singh, K. Snigdha, C. Singh, N, Sinhad and A. K. Thakur,*Soft Matter*, 2015, **11**, 5353.

37. N. D. Lourenco, J. M. Novais, and H. M. Pinheiro, *J. Biotechnol*., 2001, **89**, 163.

View Article Online
DOI: 10.1039/C9OB00014C

38. A.H. Gemeay, I.A.Mansour, R.G.El-Sharkawy and A.B. Zaki, *J. Mol. Catal. A: Chemical,* 2003, **193**, 109.

39. N. Daneshvar, H. Ashassi-Sorkhabi and A.Tizpar, *Separ. Purif. Technol*., 2003, **31**, 153.

40. E. Rindle and W. J Troll, *Journal of National Cancer Institute*, 1975, **55**, 181.

41. F.I. Hai, K.Yamamoto and K.Fukushi, *Critical Reviews in Environmental Science and Technology*, 2007, **37**, 315.

42. K L Kirk, Biochemistry of the Elemental Halogens and Inorganic Halides, 1st ed., Plenum Press, New York NY USA, 1991.

43. S. W. Zhang and T. M. Swager, *J. Am. Chem. Soc*., 2003, **125**, 3420.

44. S. Kubik, *Chem. Soc. Rev.*, 2010, **39**, 3648.

45. P. A. Gale and C. Caltagirone, *Chem. Soc. Rev.*, 2015, **44**, 4212.

46. A. P. De Silva, H. Q. N. Gunaratne, T. Gunnlaugsson, A. J. M. Huxley, C. P. McCoy, J. T. Rademacher and T. E. Rice, *Chem. Rev.*, 1997, **97**, 1515.

47. V. B. Bregovic, N. Basaric and K. Mlinaric-Majerski, *Coord. Chem. Rev.*, 2015, **295**, 9321.

48. J. Schiller, R. Pérez-Ruiz, D. Sampedro, E. Marqués-López, R. P. Herrera and D. Díaz Díaz , *Sensors*, 2016, **16**, 1.

49. T. Ghosh and B. G. Maiya, *J. Phys. Chem. A*, 2004, **108**, 11249.

50. J. Y. Lee, E. J. Cho, S. Mukamel and K. C. Nam, *J. Org. Chem.*, 2004, **69**, 943.

51. J. Lee, J. E. Kwon, Y. You and S. Y. Park, *Langmuir*, 2014, **30**, 2842.

52. P. Rajamalli and E. Prasad, *Org. Lett*., 2011, **13**, 3714.

53. B. Bai and X. Mao, *Sens. Actuators B,* 2015, **211**, 268.

54. P. Xue, J. Sun, Q. Xu, R. Lu, M. Takafuji and H. Ihara, *Org. Biomol. Chem.* 2013, **11**, 1840.

55. T. H. Kim, M. S. Choi, B. H. Sohn, S. Y. Park, W. S. Lyoo and T. S. Lee, *Chem Com.*, 2008, 2364.

56. C Baudez, R K Gupta, N Eshtiaghi, R Parthasarathy, P Slatter, Chemeca 2011: Engineering a Better World, NSW Australia, 2011.

57. M. Suzuki, M. Yumoto, M. Kimura, H. Shirai and K. Hanabusa, *Chem. Eur. J*., 2003, **9**, 348.

58. M. J. Frisch *et. al.* Gaussian 09, Revision C.01; Gaussian, Inc.: Wallingford, CT, 2010.

59. J. Tomasi, B. Mennucci and R. Cammi, *Chem. Rev*., 2005, **105**, 2999.

Figures and tables

View Article Online
DOI: 10.1039/C9OB00014C

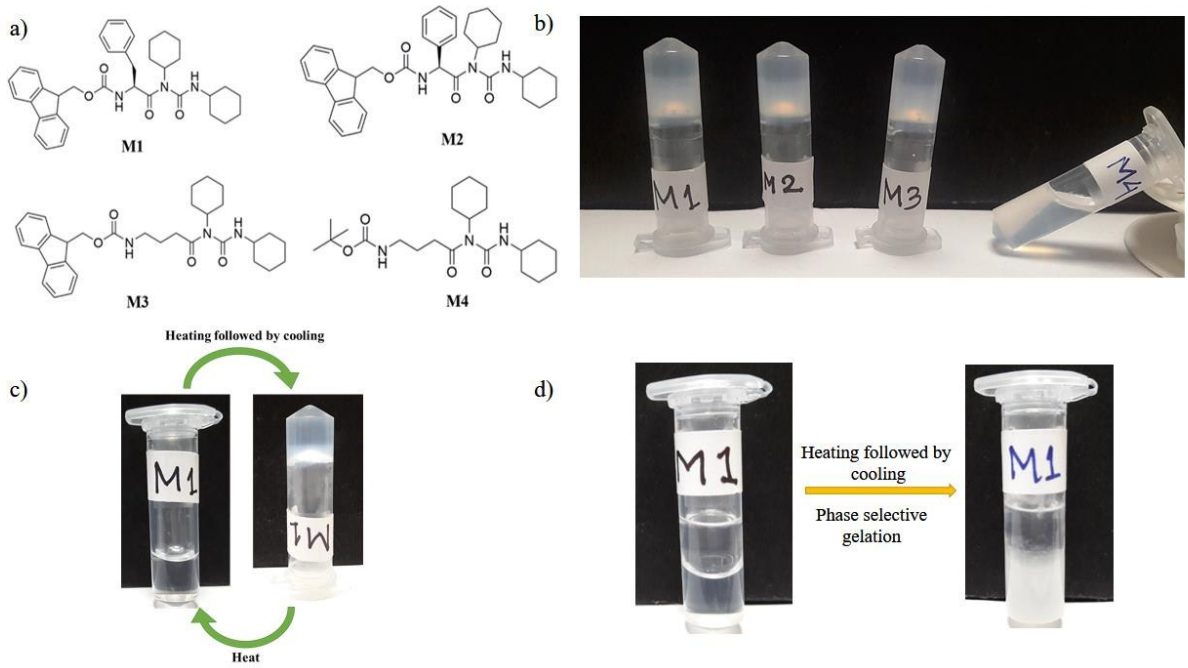

Figure 1a) Chemical structures of M1-M4.b) Gels formed from M1-M3 in 1,2 DCB . M4 does not form gel. c) Thermo-reversibility of the organogels d) Phase selective gelation behavior of the organogels.

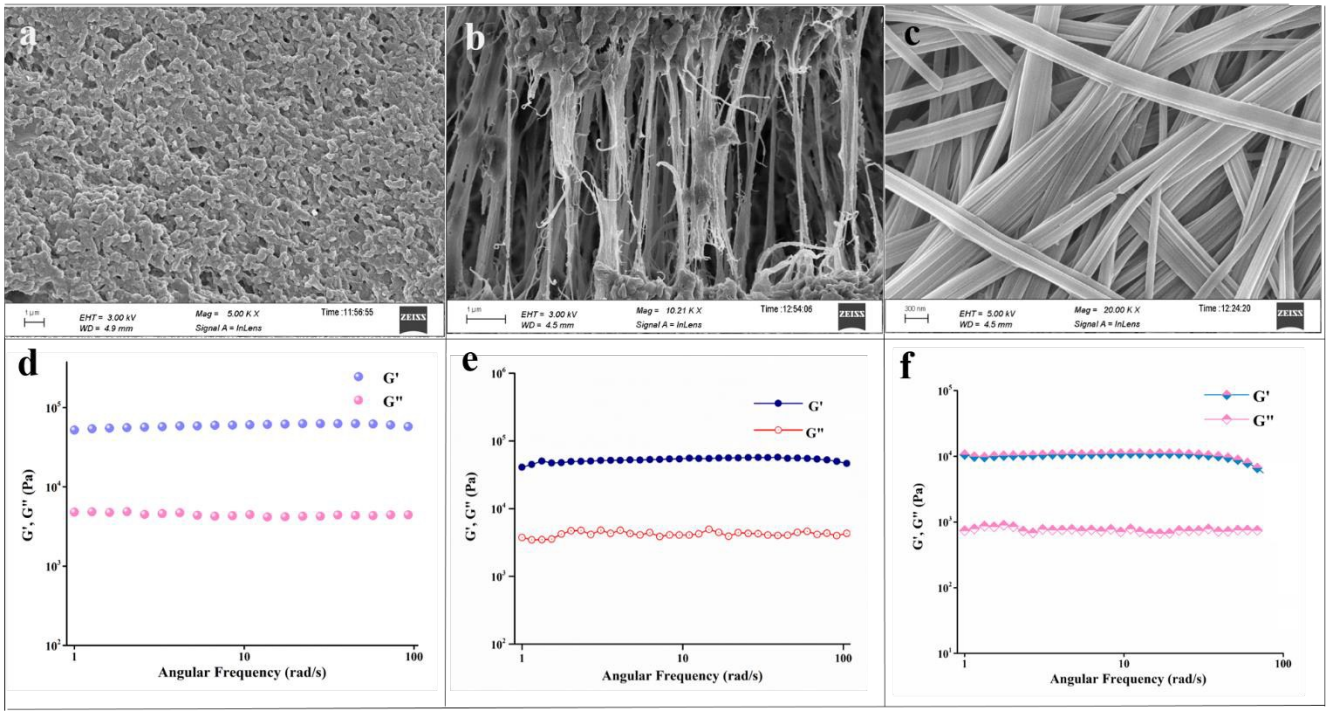

View Article Online
DOI: 10.1039/C9OB00014C

Figure 2a-c) FESEM images of the organogels formed from M1-M3 in 1, 2 DCB at their MGC. d-f) Frequency dependence of the dynamic storage moduli (G′) and the loss moduli (G″) of organogels from M1-M3 in 1,2 DCB at 2 % w/v.

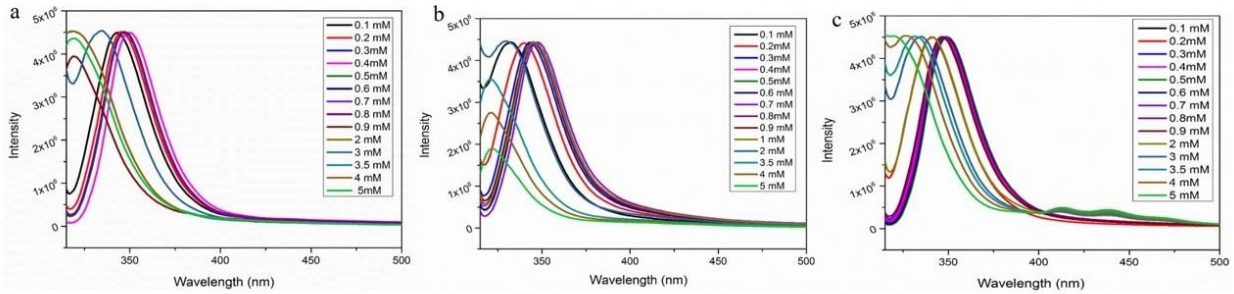

Figure 3a-c) Concentration dependent Fluorescence spectra of M1-M3 in 1,2 DCB.

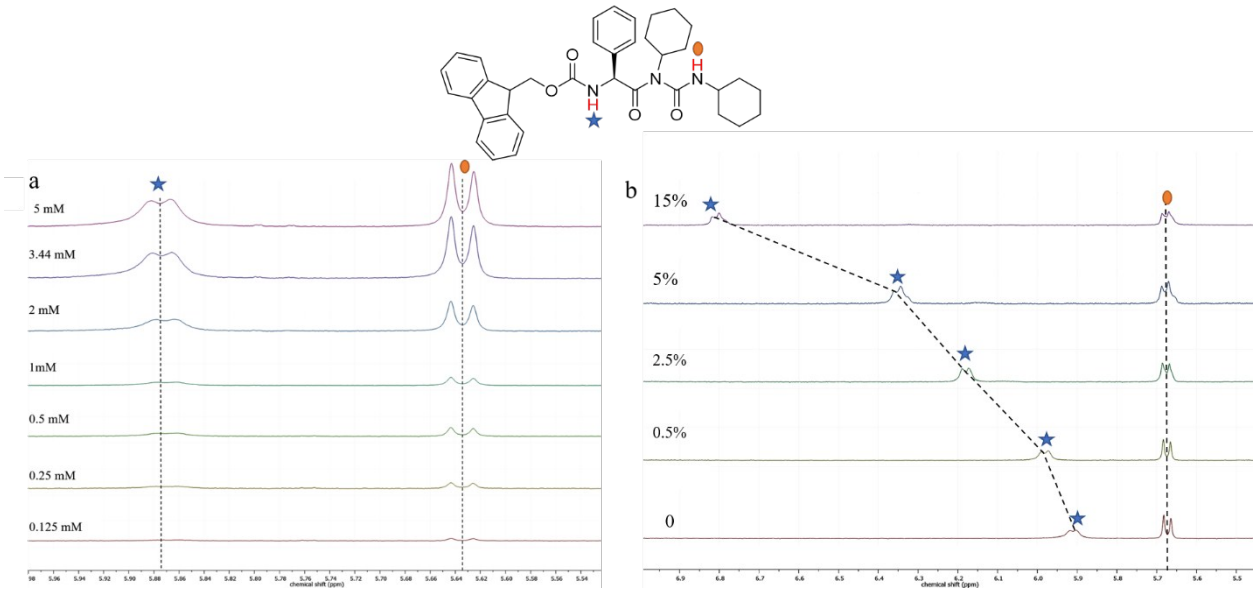

Figure 4) NH region of the stacked ^{1}H NMR spectra of M2 in $CDCl_3$ a) at different concentrations and b) at 5 mM concentration upon addition of different amounts of DMSO-d_6.

View Article Online
DOI: 10.1039/C9OB00014C

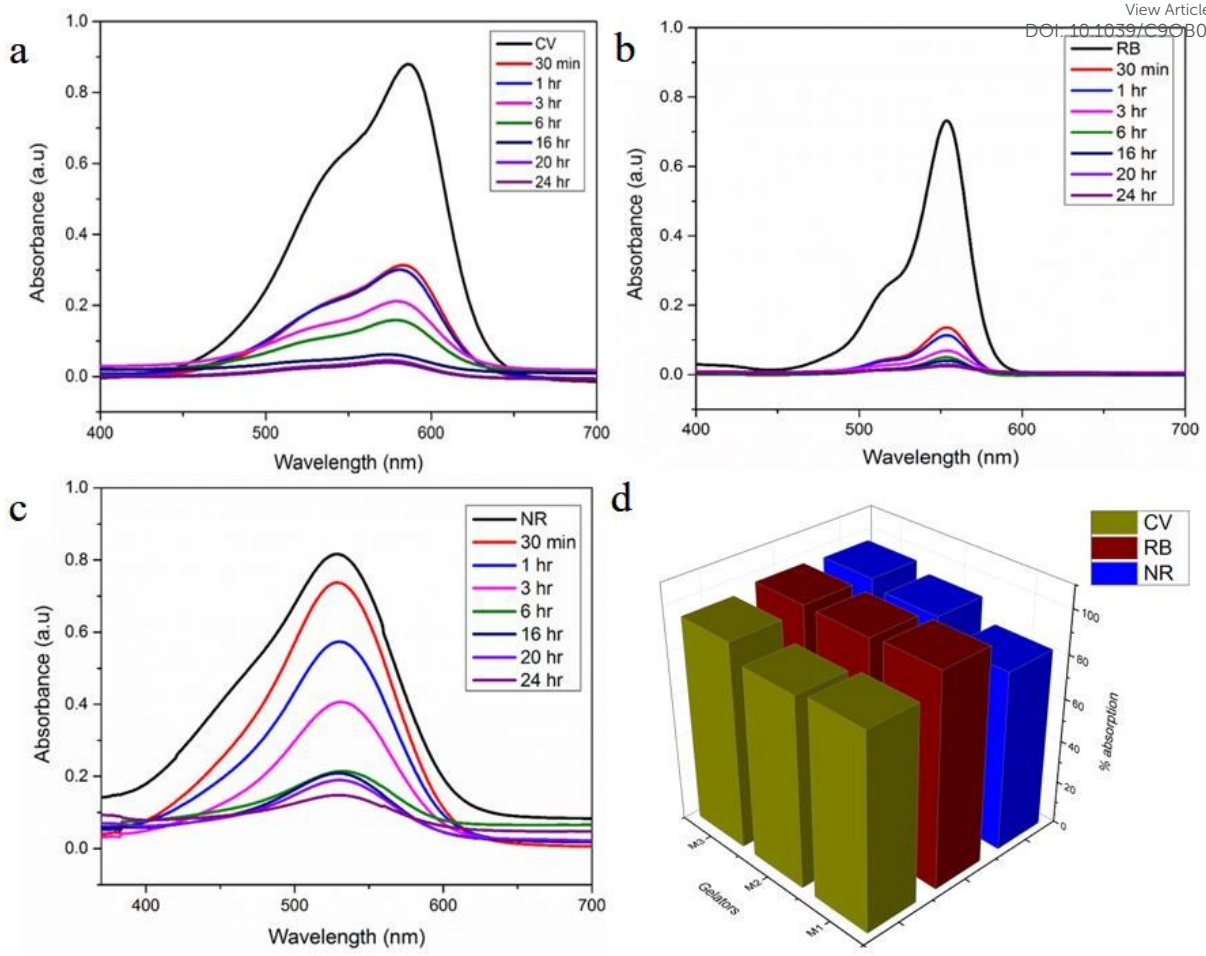

Figure 5: UV-Vis spectra showing absorption of dyes a) CV, b) RB and c) NR in the organogel formed by M1 in 1,2 DCB. d) Quantitative summary of the loading efficiency of organogels formed by M1-M3 for dyes CV, RB and NR.

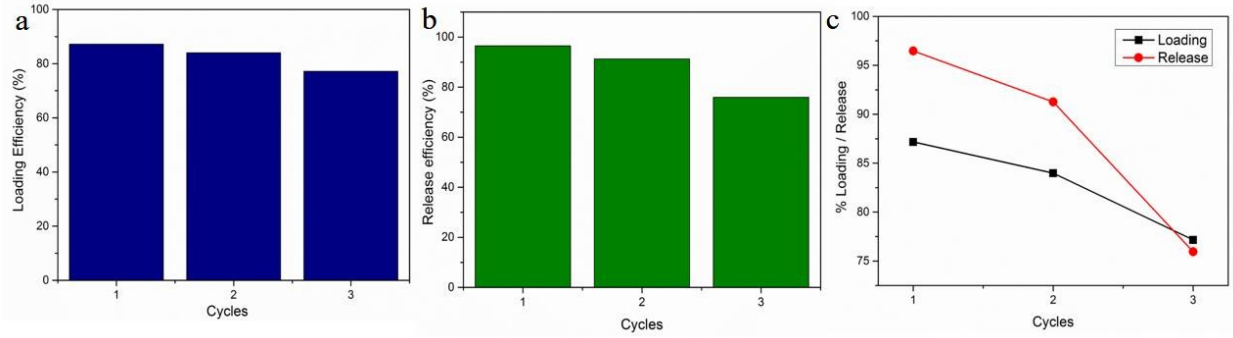

Figure 6: Reusability of organogels for dye absorption. a) % Loading efficiency of M1 organogel in 1,2 DCB in three successive cycles for dye CV. b) % release efficiency of M1 in the three successive cycles for dye CV. c) Plot of the % loading and release efficiency in three successive cycles for CV.

View Article Online
DOI: 10.1039/C9OB00014C

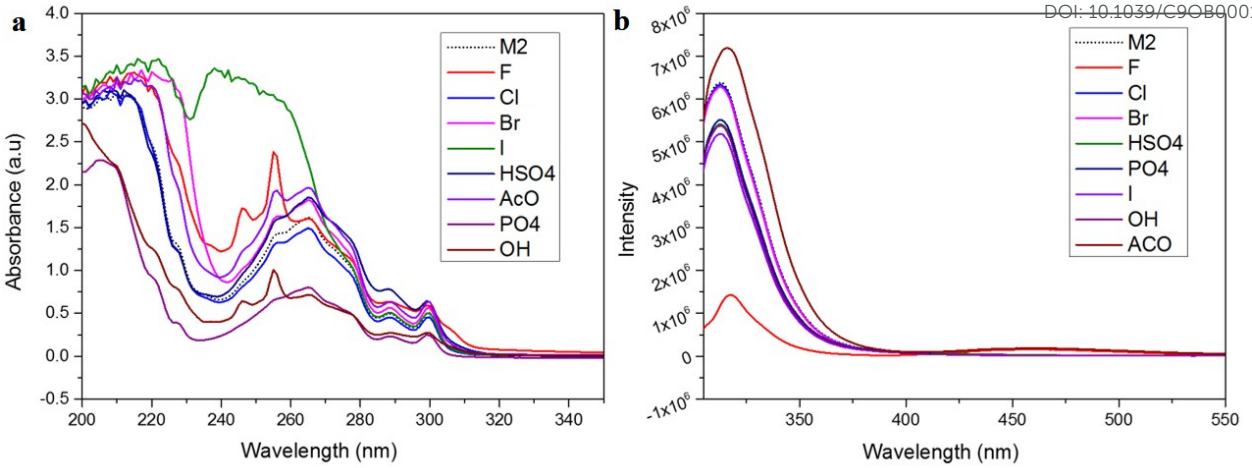

Figure 7: a) UV-Vis and b) Fluorescence spectra showing anion sensing ability of M2 in ACN (0.1 mM) for different anions (0.1 mM).

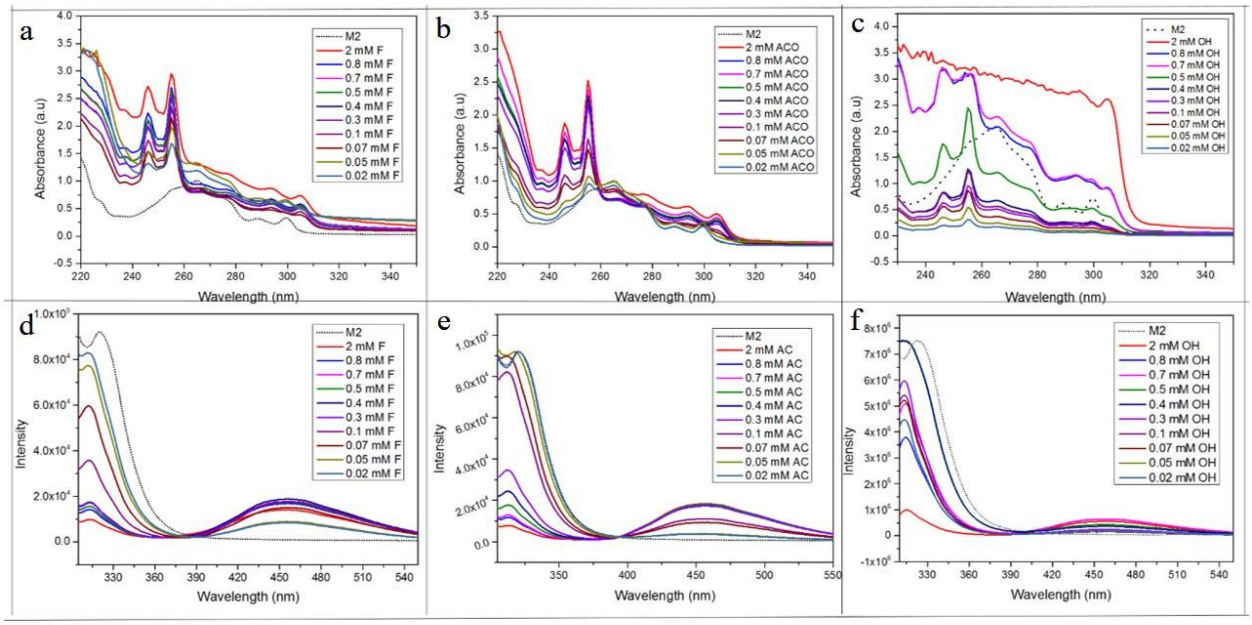

Figure8: a-c) UV-Vis spectra and d-f) Fluorescence spectra of M2 in ACN at various concentrations of anions Fluoride, acetate and hydroxide.

View Article Online
DOI: 10.1039/C9OB00014C

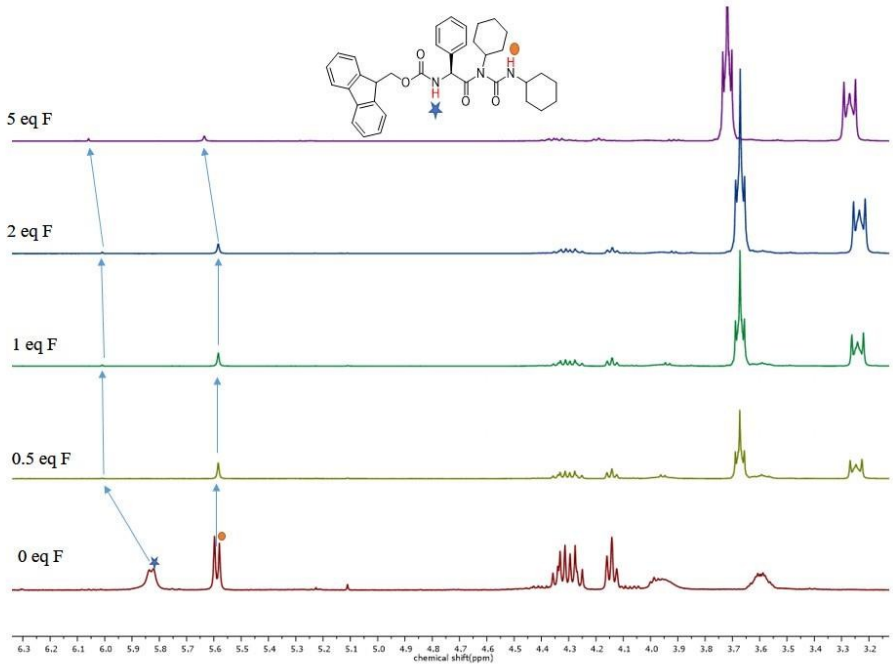

Figure 9: ^{1}H NMR titration of M2 with fluoride anion in $CDCl_3$ at room temperature.

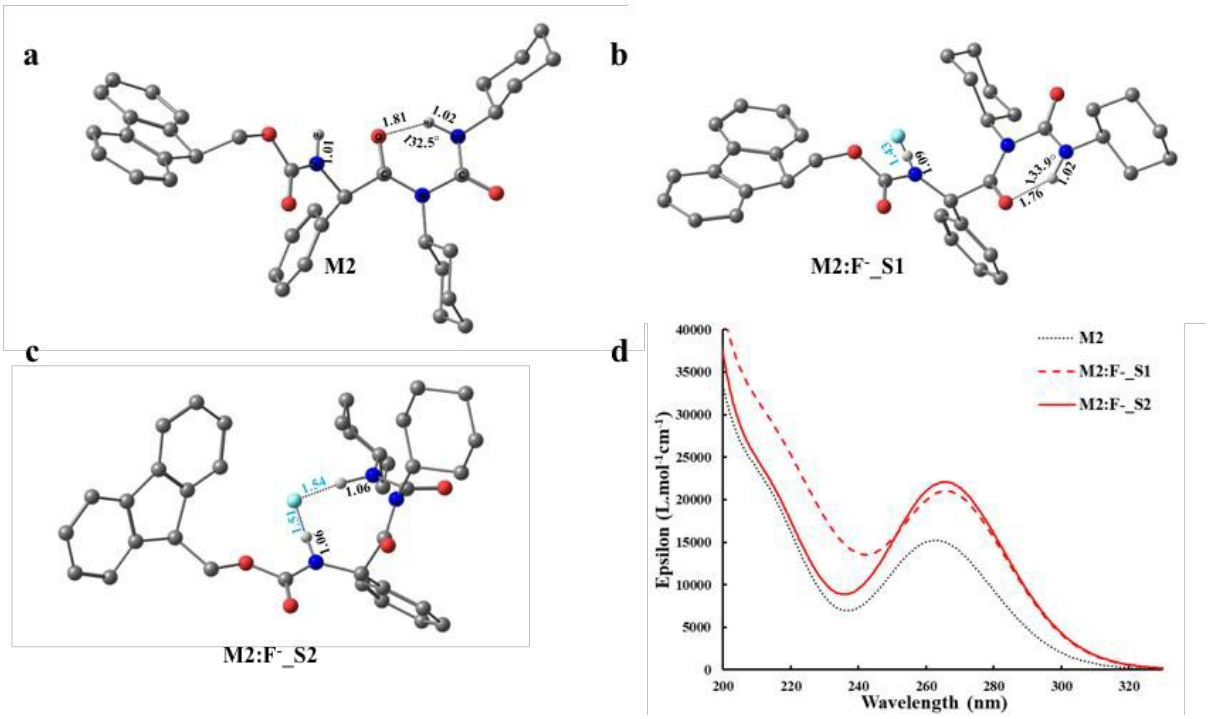

Figure 10. Optimized structures of dicyclohexyl urea derivative (a) M2 (b) Single coordinated fluoride bound complex, M2:F$^-$_S1 (c) Doubly coordinated fluoride bound complex, M2:F$^-$_S2. (d) Computed absorption spectra in ACN for M2 (dotted black line), M2:F$^-$_S1(dashed red line) and M2:F$^-$_S2 (solid red line).

View Article Online
DOI: 10.1039/C9OB00014C

Table 1: Table showing the gelation properties, physical state, MGC and sol-gel conversion temperature (T_{gel}) of M1-M3 in various solvents. OG = Opaque gel, TNS = Translucent gel, S = solution, P = Precipitate.

Solvents	M1 State/MGC(%w/v)/T_{gel}(°C)	M2 State/MGC(%w/v)/T_{gel}(°C)	M3 State/MGC(%w/v)/T_{gel}(°C)
Chloroform	OG/0.30/72	OG/0.30/70	OG/0.20/76
1,2 DCB	TNS/0.21/88	TNS/0.20/86	TNS/0.21/92
Toluene	OG/0.25/102	OG/0.25/96	OG/0.25/96
Benzene	OG/0.30/76	OG/0.30/72	OG/0.32/78
DCM	OG/0.42/30	OG/0.42/32	OG/0.40/32
THF	OG/0.35/62	OG/0.35/64	OG/0.35/68
3-xylene	TNS/0.45/86	TNS/0.45/86	TNS/0.45/90
Chlorobenzene	TNS/0.35/84	TNS/0.35/88	TNS/0.35/90
Hexane	P	P	P
Cyclohexane	P	P	P
ACN	S	S	S
Methanol	S	S	S
Diethyl ether	P	P	P
Isopropanol	S	S	S
DMSO	S	S	S
DMF	S	S	S

View Article Online
DOI: 10.1039/C9OB00014C

Table 2: The calculated absorption spectra, oscillator strengths (f) and assignments for M2, M2:F^-_S1, and M2:F^-_S2, along with experimental data.

	f value	**Assignments**	**λ_{cal} (nm)**	**λ_{exp} (nm)**
M2	0.2072	HOMO > LUMO	265.6	265
M2:F^-_ S1	0.4088	HOMO > LUMO	268.2	265
	0.0219	HOMO-2 > LUMO	254.4	255
	0.0019	HOMO-1 > LUMO	245.5	246
M2:F^-_S2	0.4343	HOMO > LUMO	267.9	265
	0.0006	HOMO > LUMO+1	255.3	255
	0.0704	HOMO-3 > LUMO+1	245.9	246